JPL PUBLICATION 82-89

Evaluation of the Potential of One to Three Seasat-SMMR Channels in Retrieving Sea Surface Temperature

Prem Chand Pandey
Stacy Kniffen

November 15, 1982

National Aeronautics and
Space Administration

Jet Propulsion Laboratory
California Institute of Technology
Pasadena, California

JPL PUBLICATION 82-89

Evaluation of the Potential of One to Three Seasat-SMMR Channels in Retrieving Sea Surface Temperature

Prem Chand Pandey
Stacy Kniffen

November 15, 1982

National Aeronautics and
Space Administration

Jet Propulsion Laboratory
California Institute of Technology
Pasadena, California

The research described in this publication was carried out by the Jet Propulsion Laboratory, California Institute of Technology, and was supported by the National Academy of Sciences and the National Aeronautics and Space Administration.

ABSTRACT

The scanning multichannel microwave radiometer (SMMR) aboard the Seasat satellite measured emitted radiation in both horizontal and vertical polarizations at microwave frequencies of 6.6, 10.69, 18.0, 21.0 and 37.0 GHz. Retrieval algorithms, for sea surface temperature (SST) determination, from subsets of one to three SMMR channels are obtained by a two step statistical technique. The technique first selects the best subsets of a given size defined by an R^2 criterion (coefficient of determination), of a given size by the application of an efficient 'leaps and bounds' technique on a statistical data base. It then performs a regression analysis on the selected subsets. The statistical data base employed a large (600) set of seasonally and geographically diverse atmospheric and surface parameters for radiative transfer calculations. The results of the study of one to three channel subset retrieval algorithms indicate the possibility of using 6.6V, 6.6H and 18V channels for SST determination from Seasat-SMMR data. A comparison of SMMR SST derived from three channels mentioned above and expendable bathythermograph (XBT) mesurements over the North Pacific provided an r.m.s. difference of ~1.4K which is comparable to the accuracy obtained from a five channel subset (6.6V, 6.6H, 10.69H, 18.0V, 21.0H) retrieval algorithm. The retrieval technique has the ability to recognize severe noise in brightness temperature measurements which may lead to unacceptable parameter retrieval. This may be achieved by setting up a quality control criteria either using different subsets of the same size or of different sizes. The three channel retrieval compares within ~1.2K with Chester's algorithm, which is being used at Jet Propulsion Laboratory for geophysical processing.

Ten day and monthly average SMMR SST contour maps are produced using three channel retrieval for the period July 7 - Aug. 6, 1978 over western North Pacific, 20-50N, 140-180E. These contour maps are compared against similar maps obtained

from Chester's algorithm and ship's observations. All the SMMR SST maps show the major climatological features and are in reasonable agreement with ship's SST maps.

CONTENTS

Figures

CONTENTS (contd)

Figures

Tables

1. INTRODUCTION

SST measurements taken from a satellite platform (which is the only practical method of covering vast oceanic regions,) are an important means for increasing our understanding of a variety of processes related to the interaction of oceans and atmospheres. For example, small surface temperature changes in the tropical regions might influence the weather in mid-latitudes, or modify such a seasonal atmospheric phenomenon as the Monsoon [Shukla, 1975]. As another example, SST monthly average fields are required for global climate monitoring [Namias, 1972]. All of these applications demand accurate and timely availability of SST data.

Because of the importance of SST, a large effort has been expended on its measurement from satellites using infrared sensors [Fritz and Winston, 1962]. These SST retrievals are degraded by the presence of clouds, although recent advances in cloud filtering techniques [Chahine, 1977, Smith, 1978], have improved the retrieval. SST retrieval using microwave sensors is less affected by the presence of clouds, due to the unique cloud penetrating capability of microwaves, although more affected by uncertainty in wind-emissivity relationships. The first experimental effort to determine SST using satellite-borne microwave radiometers, was made with the launch of Seasat in 1978. SMMR aboard Seasat and Nimbus satellites measured both horizontal and vertical polarization at narrow band microwave frequencies of 6.6, 10.69, 18.0, 21.0 and 37.0 GHz and are described in detail by Gloerson and Barath (1977) and Njoku et al (1980b). Combinations of these measurements provide information about surface and atmospheric properties with which sea surface temperature and other geophysical parameters are derived. Before geophysical processing, however, the digital data received from the satellite are processed at different stages for calibration [Swanson and Riley, 1980] and for antenna pattern correction, as described by Njoku et al (1980a). At each stage errors may be introduced which contribute to the overall errors in the

final geophysical parameters. In some instances, sun-glint and radio frequency interference effects render the data difficult to interpret [Lipes, 1980]. The proximity of land and rain in the antenna footprint also affects the SST retrieval.

To derive the geophysical parameters, all ten of the SMMR channels may be used if the observed brightness temperatures (TB's) and the geophysical models are known precisely. However, due to uncertainty in the wind-emissivity model and the known biases in TB's, these are not known precisely. These retrieval techniques assume that the parameter is homogeneously distributed within the satellite's field of view (FOV). Let us consider a FOV in which a particular parameter is inhomogeneous. As an example, scattered clouds such as the cumulus convection within the FOV of the high frequency channels which are sensitive to clouds, will not be resolved on a 54km x 54km scale. The radiometer channel will respond to the average value of the parameter which has certain variability and may be different than the true value of the parameter if the parameter would have been homogeneous within FOV. This channel if used for parameter retrieval will affect the retrieval accuracy by way of providing errors in the bias. Thus, to derive a given geophysical parameter, one should heavily weight those channels which are most sensitive to that parameter and less sensitive to other atmopsheric parameters. Using a small number of channels to retrieve a given geophysical parameter minimizes the sensitivity of the algorithm to channel dependent biases. No previous attempts have been made to evaluate the suitability of one, two or three channels to retrieve SST from Seasat SMMR data, although efforts to retrieve water vapor and liquid water from two channels have successfully been made from earlier Nimbus satellites [Grody, 1976, Staelin et al 1976]. Hofer et al (1981) used five channels to retrieve SST from Seasat-SMMR data by the application of a forward regression method on a statistical data base. In a previous paper, the

authors [Pandey and Kakar, 1982a] developed a two-step statistical technique for retrieving a given geophysical parameter from multiwavelength measurements and examined subsets of four to ten radiometric channels for SST estimation. We present in this paper, results of the evaluation of the effectiveness of the best one to three channel subsets of SMMR for SST retrieval. The SMMR-SST's are compared with in situ XBT-SST observations and also with the results of Chester's algorithm [Lipes and Born, 1981]. A brief summary of Chester's algorithm is given in the Appendix. The SMMR-SST fields (contour maps) obtained from three channels are compared with ships' SST climatology fields on a monthly and ten day average basis for the period July 7 - Aug. 6, 1978 over the Pacific, 20°-50°N, 140°-180°E.

2. Retrieval Algorithm

Retrieval techniques described in the literature include, among others, statistical [Waters et al 1975, Grody, 1976, Wilheit and Chang, 1980, Pandey et al, 1981, Hofer and Njoku, 1981, Pandey and Kakar, 1982a], non-linear iterative [Wentz, 1982], and fourier transform techniques, the latter developed by Rosenkranz (1978). The retrieval equations discussed and used here have been derived using a two-step statistical technique described in detail by Pandey and Kakar (1982a). The technique is based upon the application of an efficient algorithm, known as 'Regressions by leaps and bounds' [Furnival and Wilson, 1974], to a statistical data base in order to select the 'best' subsets of radiometric channels. The 'best' is defined using the R^2 coefficient of determination criterion, widely used in statistical literature. Our approach is unique, in the sense that it provides an opportunity to examine a number of subsets and also different subsets of the same size, which is not possible by other methods. The statistical data base consists of an ensemble of realistic sea surface temperatures, wind speeds, atmospheric water vapor profiles, temperature profiles and cloud models and are summarized in Table 1. Our approach to generating the data base is also slightly different than that used by earlier investigators. We have used a non-linear regression equation between water vapor and SST, which exist in nature, to generate the data base, along with other parameters. This relation was obtained from the analysis of water vapor and SST data obtained from ocean station PAPA (50°N, 145°W) and the Monex '79 experiment. The analysis gave a value of 0.77 for the coefficient of correlations. These are used to calculate brightness temperatures by means of a surface emission model [Pandey and Kakar, 1982b] and a radiative transfer model. The retrieval equations are then obtained by using multiple linear regression on the selected subsets, based upon the statistical relationship between geophysical parameters and the calculated brightness temperatures. Non-linearity of the problem was

TABLE 1. Range of environmental parameters used in generating theoretical brightness temperatures. Integrated water vapor (WV) includes correction due to saturation within clouds. Cloud density set to zero for atmospheric temperature <-40°C.

Model Atmosphere	Weather Specification	Number	Range of Parameters				
			SST K	WS m/sec	WV g/cm^2	LW g/m^3	RR mm/h
Annual Tropic	clear	93					
	cloud	57	286-310	0-35	2.7-7.51	0-.55	0-2.5
	rain	12					
Sub Tropical	clear	97	273-307	0-35	0.8-8.33	0-.45	0-5
	cloud	53					
	rain	31					
Mid Latitude	clear	97	273-307	0-35	0.8-6.11	0-.45	0-3.5
	cloud	53					
	rain	31					
Sub Arctic	clear	111	271-292	0-35	0.6-5.33	0-.25	0-3.5
	cloud	39					
	rain	17					

mitigated by using functions of brightness temperature [$f(T_B) = \ln (280-T_B)$] in lieu of brightness temperatures themselves, for high frequency (18.0, 21.0, 37.0 GHz) channels. Theoretical brightness temperatures were perturbed by Gaussian noise, characteristic of the SMMR instruments, which smoothed the regression coefficients and provided a more realistic approach to the problem.

The flow diagram of the leaps and bounds procedure is given in Fig. 1. In the on-line part of the flow diagram, the quality control criterion is shown for sea surface temperature as an example and may be replaced for other parameters and either the same or a different quality-control criterion can be set up. The threshold value of the parameter for quality control will depend upon the parameters being estimated and the accuracy obtainable from such measurements.

We have further studied the effect of nonlinearities in the above equations by using second order regression relations. These relations have the same form as given earlier, except that the squares of the measured brightness temperatures are included as predicting observations. Thus, the number of predictor variables in the regression equations are doubled.

The results of the leaps and bounds algorithm for selecting the best subsets of 1 to 3 channels are given in Table 2 along with the R^2 values. As an example, the second best subsets are also given and may be used for analysis as well. This capability could be exploited to set up a quality control criteria in future algorithms as proposed in the earlier paper [Pandey and Kakar, 1982a]. Table 3 gives the regression coefficients for the selected best subsets, including linear and nonlinear equations. The coefficients in Table 3 are related with brightness temperatures by the following relations:

$$SST(P) = a_0 + \sum_{i=1}^{p} a_i \, T_B(\nu_i) + \sum_{i=1}^{p} b_i \, T_B^2(\nu_i)$$

where p is the size of the subset, a_0 is the intercept and a_i's are the

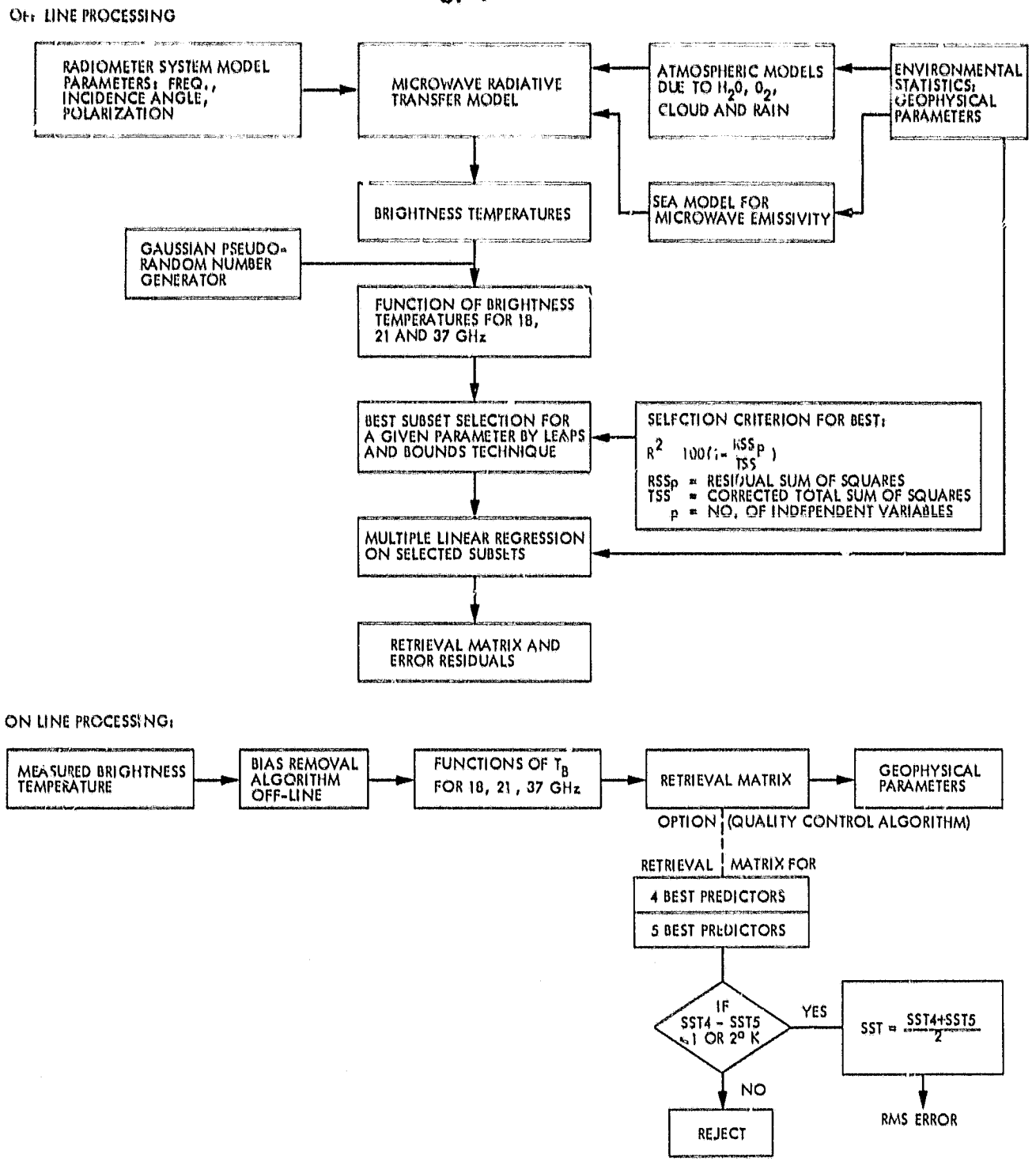

Fig. 1. Logical flow diagram showing the development of two step statistical inversion algorithm

TABLE 2. Output of the leaps and bounds technique for selecting 'best' subset of sizes 1 to 3. The second best subset is also shown as an example.

No. of Variables for Regression	R^2	Variables Selected
1	75.71	6.6V
	34.19	10.6H
2	93.34	6.6V, 10.6H
	92.62	6.6V, 10.6V
3	94.97	6.6V, 6.6H, 18.0V
	94.83	6.6V, 18.0V, 21.0V

TABLE 3. Coefficients of the multiple linear regression on the selected best subsets given in Table 1.

Channels	Type of Regression	Regression Coefficients		r.m.s. error (K)	R^2
6.6V	linear	a_0	68.9391		
		a_1	1.4436	4.5	75.71
6.6V, 10.6V	linear	a_0	31.8548		
		a_1	2.8115		
		a_2	-1.0533	2.40	93.34
	non-linear	a_0	-505.2264		
		a_1	8.6364		
		a_2	.0537		
		b_1	-.0195		
		b_2	-.0028	2.01	95.35
6.6V, 6.6H, 18.0V	linear	a_0	-103.1898		
		a_1	2.4618		
		a_2	-.5687		
		a_3	15.2752	2.08	94.97
	non-linear	a_0	-185.9112		
		a_1	3.0475		
		a_2	2.9708		
		a_3	-41.2869		
		b_1	-.0023		
		b_2	-.0182		
		b_3	6.4685	1.57	97.17

regression coefficients and $T_B(\nu_i)$'s are the brightness temperatures for 6.6 and 10.69 GHz frequencies and functions of brightness temperature for 18, 21 and 37 Ghz channels as described earlier. The b_i's coefficients are multiplied by the square of either Tb's or functions of T_B, depending upon frequencies for non-linear regression analysis. The theoretical r.m.s. error is also shown in the Table. It should be pointed out here that the theoretical r.m.s error is dependent upon the range in variations of geophysical parameters used in the statistical data base and should not be directly compared with r.m.s. error obtained by other investigators.

3. Results of comparisons over the North Pacific:

3.1 Comparison with in situ SST measurements and Chester's algorithm.

The Seasat-SMMR data for September 14-26, 1978, over the North Pacific, were used for comparison with in situ SSTs measured by XBTs. The ground truth XBT measurements are inherently accurate to better than ~0.2°C, but the time difference between the satellite pass and the ships' observations, a difference of about one day, introduces additional noise to the in situ measurements. Moreover, additional uncertainty is introduced because of different sampling characteristics of SMMR and XBT observations. This may further compound the problem if the actual SST has significant horizontal gradients. These aspects should be kept in mind while comparing satellite derived SST with in situ SST observations. The results of the comparison are shown in Table 4. The r.m.s. error and bias are also given in the Table. The subset of channels 6.6V, 6.6H, and 18.0V gives the minimum r.m.s. error of ~1.4K which compares well with the r.m.s. error obtained earlier [Pandey and Kakar, 1982a] using a subset with five channels. Non-linear effects have also been studied and the results are presented in Table 4. The single channel retrieval gives an rms error of 2.03K with a bias of -3.89K. The bias and retrieval error using non-linear terms was not attempted for the

TABLE 4. Results of the SMMR-SST Versus in situ XBT/AXBT-SST analysis for descending passes over North Pacific region. Bias is the difference between SMMR-SST and XBT-SST.

Subset Size	Channels	RMS Error (K)		Bias (K)	
		Linear	Non-Linear	Linear	Non-Linear
1	6.6V	2.03	-	-3.89	-
2	6.6V, 10.69V	1.75	1.72	7.81	6.38
3	6.6V, 6.6H, 18.0V	1.40	1.56	0.10	1.86
5	6.6V, 6.6H, 10.60H, 18.0V, 21.0H	1.43	-	-	-

single channel case because of the known poor retrieval accuracy (~4.5K) of a single 6.6 GHz channel as obtained from a simulated theoretical data base and presented in Table 3. The comparison with a 5 channel subset was made after correcting biases (~6K) which were obtained by comparison of Seasat SMMR SST with XBT-SST measurements obtained over the North Pacific.

No improvement is obtained over linear retrieval (Table 4). However, non-linear retrieval from a statistical data base showed some improvement (Table 3). It is interesting to observe that linear regression equation for three channels has almost negligible bias and thus may be used for Seasat SMMR SST retrieval. This is probably due to the fact that bias in the individual channels and/or combinations of channels has a nullifying effect on the other's offset. Figure 2(a) shows the plot of SMMR SST obtained using a three channel subset (6.6V, 6.6H, and 18.0V) and in situ measurements. An r.m.s. difference of ~1.4K was obtained with negligible bias. The temperature range was ~10°-30°C. Figure 2(b) shows the plot of residuals versus predicted SST. Random scatter around the mean line reflects the aptness of the model for retrieving SST. The advantage of using a small number of channels is that the effect of multi-collinearity, which may be present if all channels are used, is minimized. The problem of multi-collinearity has been discussed in many statistical texts. If high multi-collinearity is present the following problems may occur (Green and Carrol, 1978):

1. Reduced precision in estimating the coefficients of predictive functions and increased difficulty in disentangling the separate effects of each predictor variable on the criterion variable, may take place.
2. Estimation of regression coefficients may become highly sensitive to a specific sample; addition or deletion of a few observations can produce marked differences in the values of the regression coefficients including changes

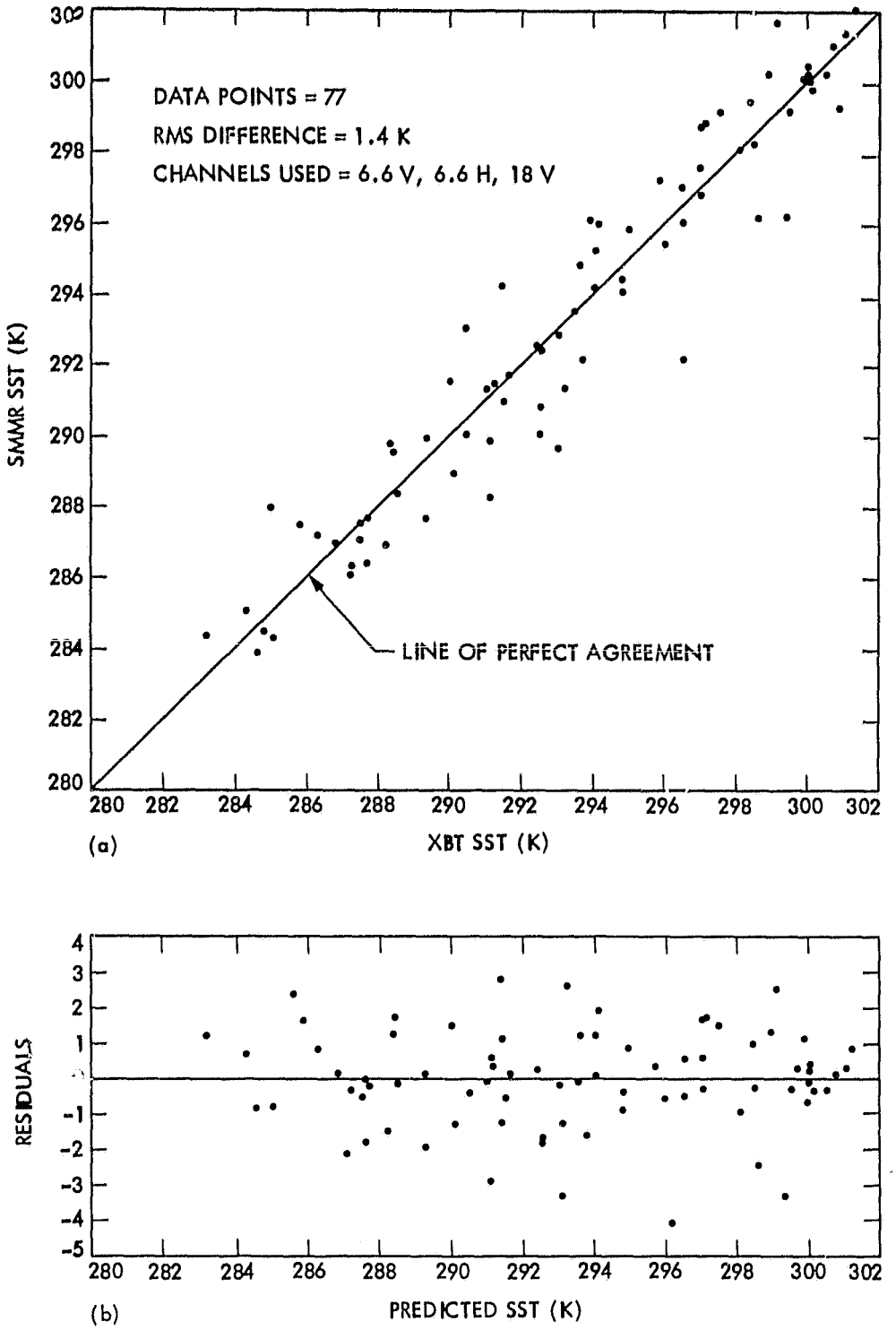

Fig. 2. (a) Comparison of SMMR-SST with XBT-SST observations for descending Seasat revolutions over the North Pacific for the month of Sept. 1978

(b) Residual plot for the predicted values of SST

in algebraic sign. Unfortunately some collinearity will always be among the predictor variables, but the question is how much multi-collinearity can be tolerated without seriously affecting the results. Unfortunately there is no simple answer to this question. Using the minimum number of channels helps, perhaps, to reduce the multi-collinearity problem.

Figure 3 shows the plot of SMMR-SST retrieval using 3 and 5 channels. The five-channel retrieval was corrected for the bias using the method described earlier by Pandey and Kakar (1982a).

Table 5 gives the results of the comparison of SMMR-SST retrieval using subsets of 1, 2 and 3 channels to the results of Chester's algorithm [Lipes and Born, 1981]. Two hundred data points from grid 1 (spatial resolution ~150 km^2) and columns 1-3 were used for comparison. These data spanned from the equator to ~50° Latitude in the North Pacific region. As can be seen from Table 5, both Chester's and the present algorithm using 2 and 3 channels for both linear and nonlinear terms, agree within an r.m.s. error of ~1K with a bias of ~1K for 3 channel retrieval. Even retrieval with the single 6.6V channel gives an r.m.s. error of ~1.5K. The plot of SMMR-SST from the present three channel retrieval and Chester's algorithm are shown in Fig. 4. The plot shows a rotation of the regression line about ~290K which could be corrected empirically by comparing a large number of high quality in situ observations covering a wide geographic area. Chester's algorithm incorporates this correction. This has not been attempted in the present analysis as we did not observe this behavior in our comparisons over the North Pacific. This correction may be more noticeable for very low (<280K) and very high temperature (>300K).

3.2 Description and comparison of SMMR-SST maps against ships' SST maps.

The previously mentioned capability of SMMR-SST retrieval using three channels, has been further investigated by comparing SST maps generated from

TABLE 5. Results of the comparison of SMMR-SST derived using present algorithm with Chester's algorithm.

Subset Size	r.m.s. error (K)		Bias (K)	
	Linear	Nonlinear	Linear	Nonlinear
1	1.52	-	-3.25	-
2	1.12	1.13	7.27	6.33
3	1.15	1.15	0.97	2.51
5	1.54	-	-	-

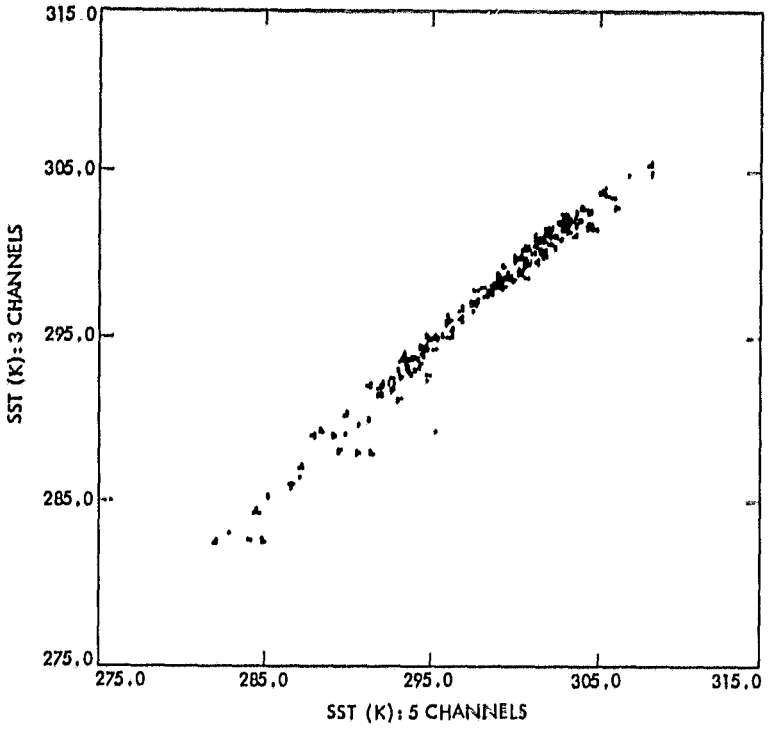

Fig. 3. Comparison of SMMR-SST derived using three and five SMMR-channels

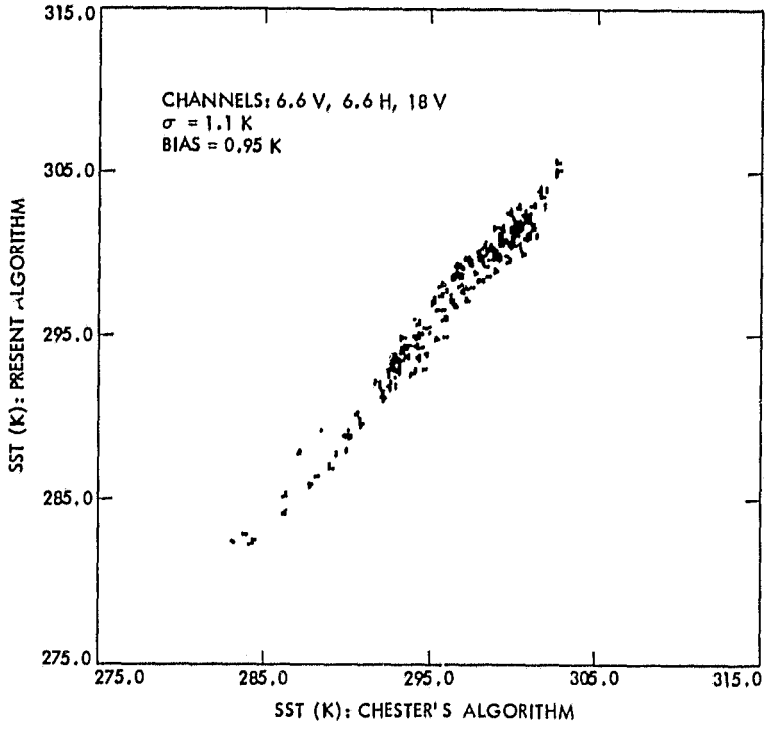

Fig. 4. Plot of SMMR-SST derived using present algorithm with three channel subset (6.6V, 6.6H, 18V) versus Chester's algorithm

SMMR data against SST maps generated from in situ ships' reports [Bernstein, 1982] and SST maps produced by using Chester's algorithm. We have used the period from July 7 to August 6, 1978, for SST mapping. The data analysis region and period are the same as used by Bernstein (1982) for ease of comparison, but the mapping procedures are different. In our approach, the brightness temperature data were used to obtain SST using a linear 3-channel algorithm as described earlier. These parameters were then interpolated for a fixed 2°x2° latitude-longitude grid extending from 20°-50°N, 140°-180°E, for further analysis. Since the algorithm is applicable only to sea surfaces, any data near land will produce error and should be avoided. The interpolated values of SST at each grid point were obtained using a weighted average of all data within a 2° radius of influence for each grid point according to

$$SST = \frac{\sum W_i \ SST_i}{\sum W_i} \qquad (1)$$

The weighting factors W_i assigned to the individual data values are given by the Cressman formula

$$W_i = \frac{D^2 - d_i^2}{D^2 + d_i^2} \qquad d_i < D$$
$$= 0 \qquad d_i > D$$

where D is the 2° radius of influence and d is the distance of the data points from the grid position. The uniform grid of SST created by this weighting process was used as input for the contour package. The software used to generate these contour plots was developed by Chelton at Jet Propulsion Laboratory and implemented on a Digital VAX 11/780 using the Pilot Ocean Data System. It should be noted that Chelton's program uses a "box filter" method of smoothing the data in which the contents of a box surrounding the point of interest are averaged to derive a new grid point value. In the contour plots presented here a 6°x2° box filter was

used (Figures 5, 7, 8(a), and 8(b)).

The SMMR data (Table 6) were blocked into three consecutive 10 day intervals and the maps were produced. The SMMR-SST fields are displayed in Figure 5. Figure 6 shows the SST fields obtained from ships' data [Bernstein 1982]. Some difference between the two fields is noticeable particularly in data sparse regions, but the major features of both the fields are in overall agreement. Both fields show a strong gradient around 40° and agree reasonably well in terms of gradient intensity, direction, extent and absolute magnitude. The isotherm contour obtained from SMMR data does not show wavy-like structure as displayed by isotherms obtained from ships' observations. Bernstein (1982) attributes this "bulls-eye" feature to internal inconsistency of neighboring ships' reports. A careful examination of ships' reports might reveal more insight into this aspect. Figure 7, which is similar to Figure 5, displays the SMMR-SST field obtained by Chester's algorithm, using 3-channels. This method of comparing contour plots avoids the discrepancy which might arise by using different mapping procedures.

In order to suppress the noise further, we have produced an average monthly map by combining the data. This map is shown in Figure 8 along with the monthly SST maps obtained from ships' observations and from Chester's algorithm. The noise in the isotherm is now much reduced but some of the irregularity in ships' SST fields is still there. Again, the major features are in reasonable agreement in all SST fields. Figure 9 shows the long term average of the SST fields for the month of July which was obtained by using the Surface II Mapping Procedure described by Bernstein (1982). Our monthly SST map compares favorably with this long term SST map.

4. Conclusions and Remarks

The results of the present study indicate the possibility of using three

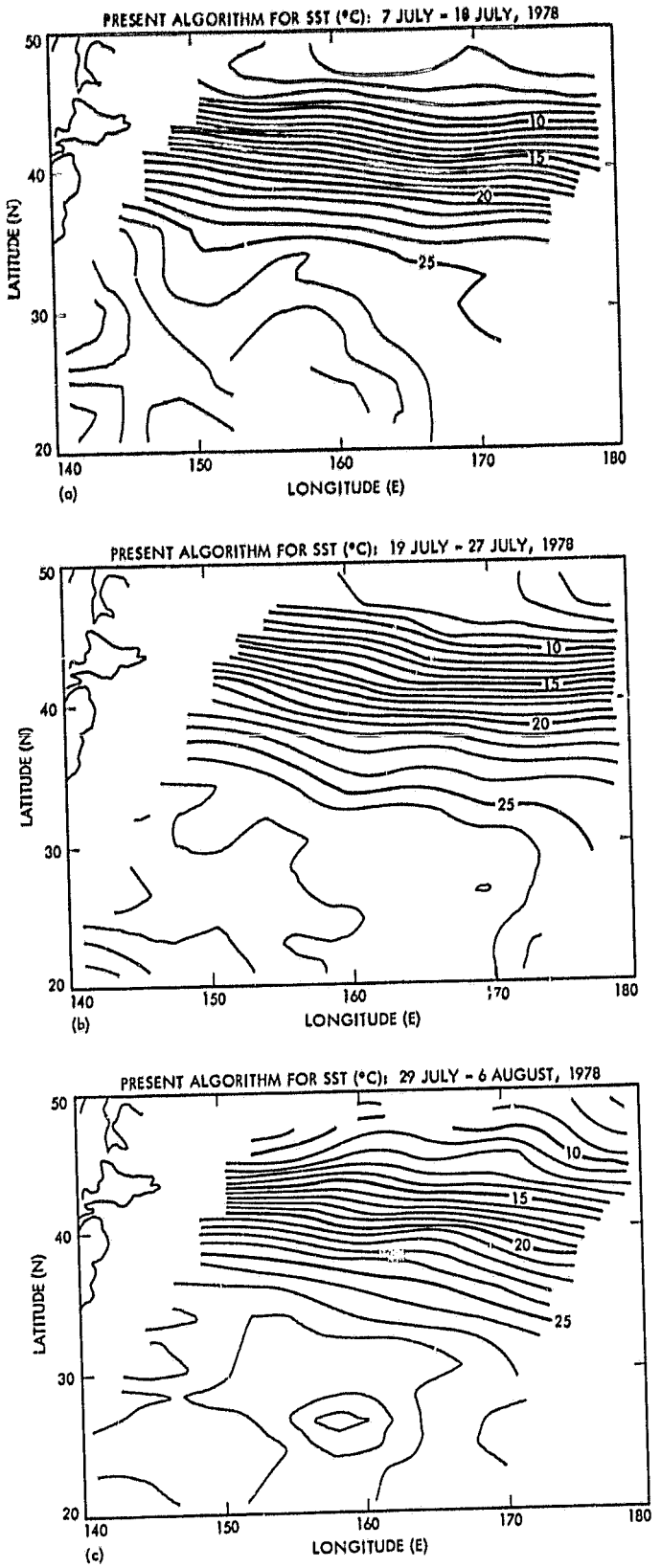

Fig. 5. SMMR-SST field for three 10-day intervals in the Western midlatitude North Pacific, using present algorithm with 3-channel subset

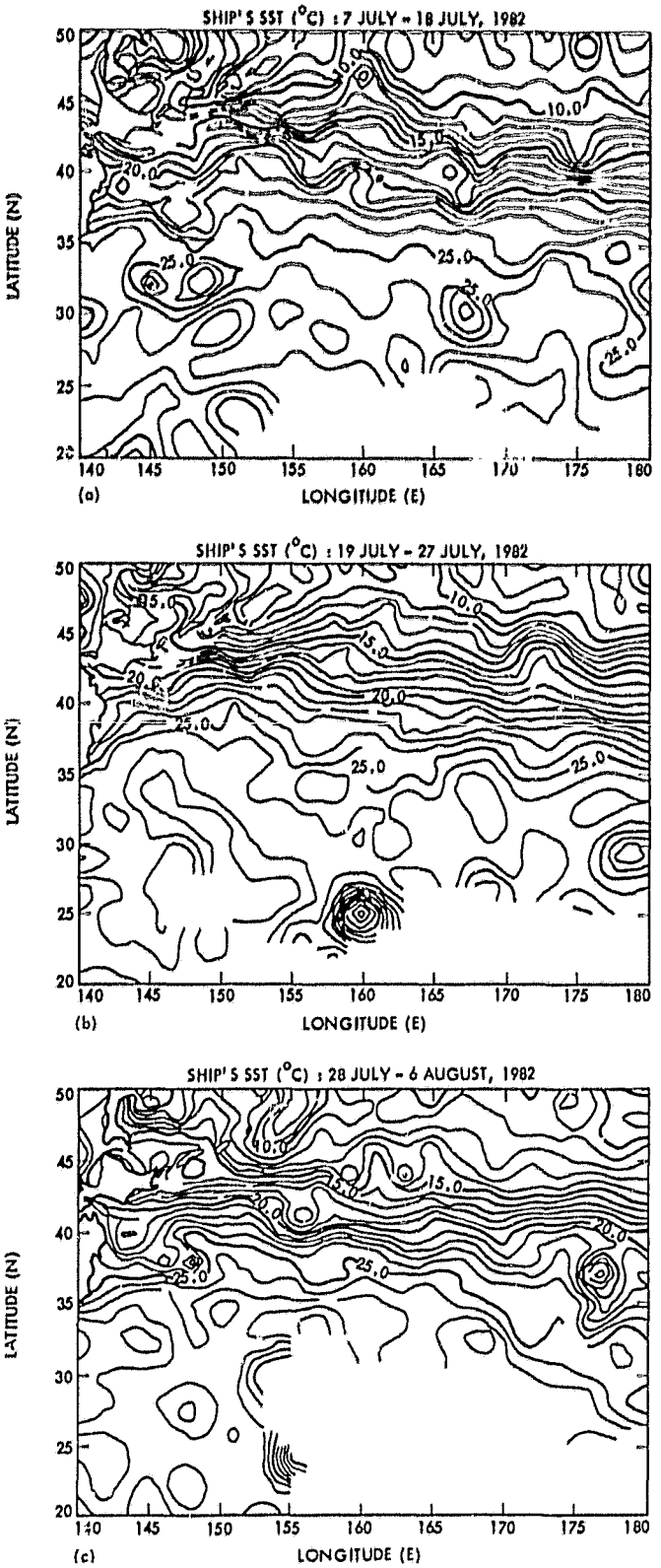

Fig. 6. SST field obtained (from Bernstein, Scripps Institute of Oceanography 1982) from ships' observations using different mapping procedures

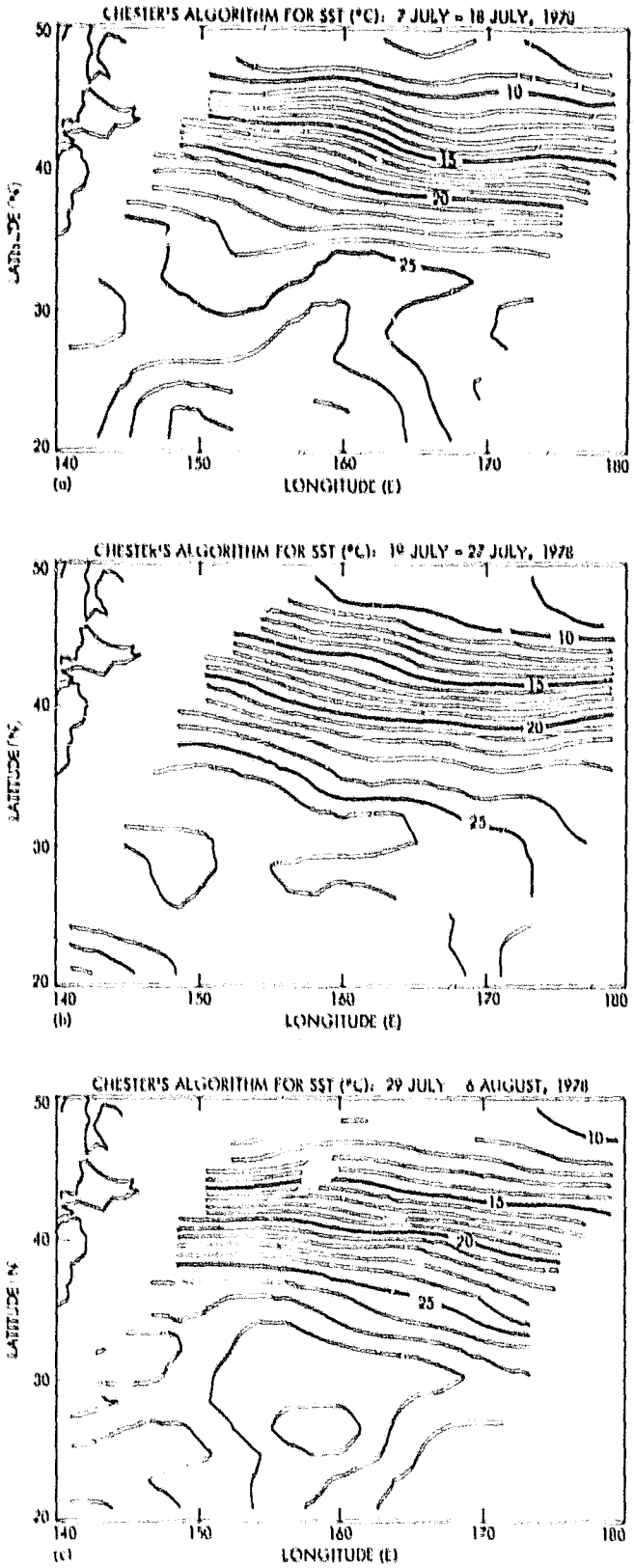

Fig. 7. SMMR-SST field for three 10-day intervals in the Western midlatitude North Pacific, using Chester's algorithm. Mapping procedure is the same as in Fig. 5

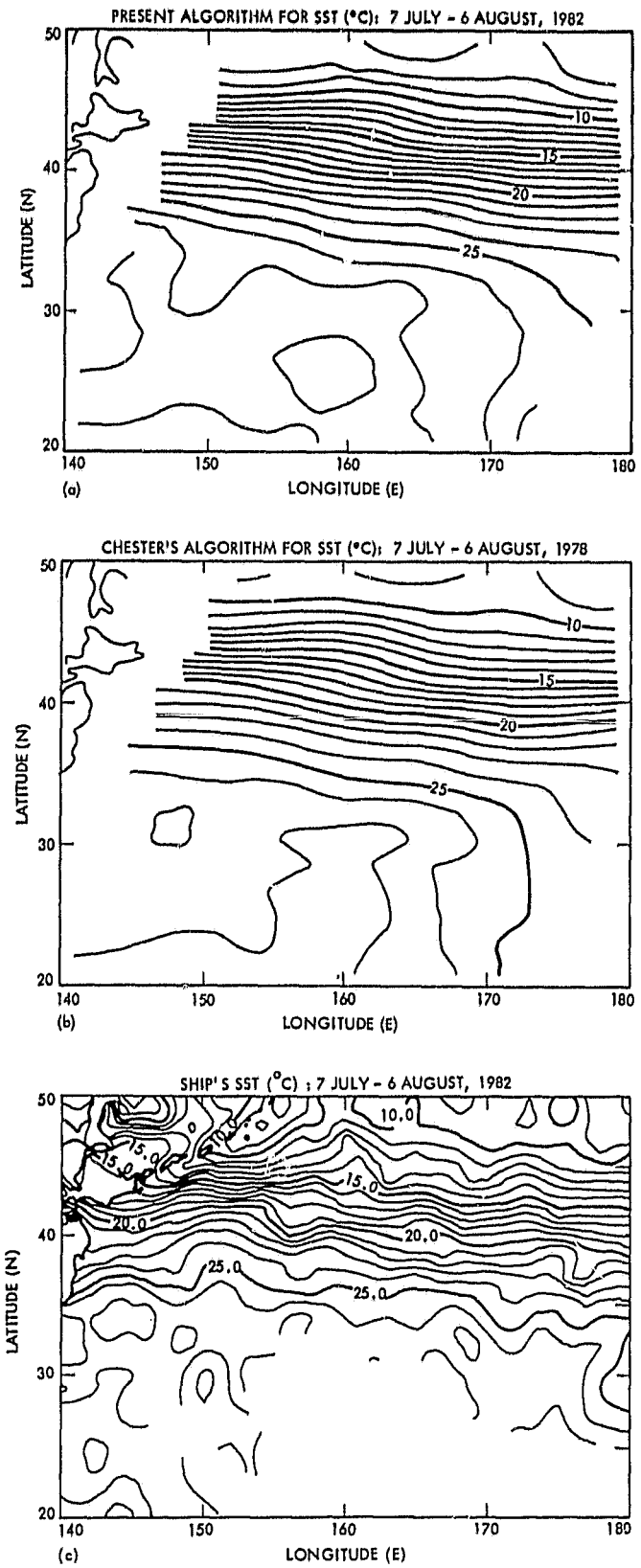

Fig. 8. Monthly field of SST obtained from, (a) present 3-channel subset, (b) Chester's algorithm (c) ships' observations (from Bernstein, Scripps Institute of Oceanography, 1982)

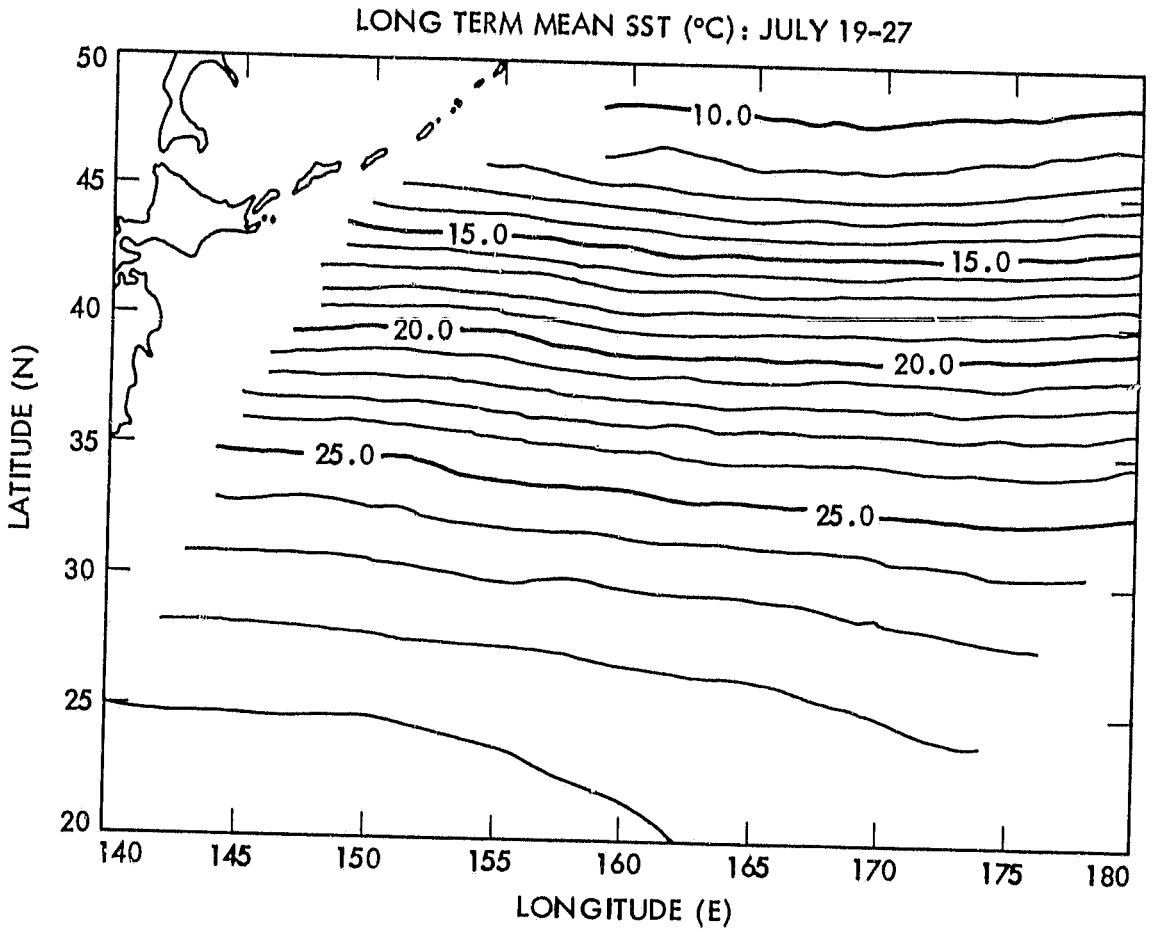

Fig. 9. 20-year mean sea surface temperature climatology (from Jerome Namias, Scripps Institute of Oceanography)

TABLE 6. Summary of the Seasat revolutions used in generating the SST fields.

Orbit No.	Date	Times	Equator Crossing °E
147	7 July 78	0744-0754	137.8
175	9 July 78	0639-0650	155.5
204	11 July 78	0718-0727	148.1
218	12 July 78	0648-0652	156.9
233	13 July 78	0756-0807	140.6
262	15 July 78	0834-0845	133.3
276	16 July 78	0803-0814	142.1
290	17 July 78	0733-0735	151.0
304	18 July 78	0701-0712	159.8
319	19 July 78	0810-0821	143.5
333	20 July 78	0737-0753	152.4
458	21 July 78	0848-0902	136.1
362	22 July 78	0816-0831	145.0
376	23 July 78	0745-0759	153.8
390	24 July 78	0713-0727	162.6
391	24 July 78	0854-0908	137.6
405	25 July 78	0824-0838	146.4
419	26 July 78	0752-0806	155.2
433	27 July78	0720-0734	164.1
434	27 July 78	0901-0915	139.0
462	29 July 78	0759-0813	156.7
477	30 July 78	0909-0922	140.5
505	1 Aug 78	0806-0820	158.1
520	2 Aug 78	0915-0930	141.9
534	3 Aug 78	0845-0859	150.7
548	4 Aug 78	0813-0828	159.6
549	4 Aug 78	0953-1007	134.5
563	5 Aug 78	0922-0936	143.4
577	6 Aug 78	0851-0906	152.2

channels for SST determination. Theoretical retrieval accuracy of ~2K is achievable as shown in Table 3. The advantages of this approach are the reduction of the bias problem, and reduction of the cost of instrumentation for future satellites. The maps of SST fields produced with three-channel retrievals compare well with SST fields obtained by using ships' observations over the North Pacific and display the major climatological features. Moreover, the SMMR-SST comparison reported in the present paper between three-channel and five-channel retrieval shows reasonable agreement. However more comparisons with varied atmospheric conditions, at different geographical locations and times, are needed to determine the validity of the algorithm for global SST predictions. Also, more subsets should be examined with actual SMMR data to determine the suitability of the subsets for SST retrieval. This will also provide the opportunity to evaluate the effectiveness of other SMMR channels in retrieving SST.

ACKNOWLEDGEMENTS

J. W. Waters, E. G. Njoku and R. K. Kakar are gratefully acknowledged for their valuable comments on the manuscript. R. L. Bernstein of Scripps Institute of Oceanography, La Jolla, California provided useful comments on the contours presented in this manuscript. Dudley Chelton provided his software package for contour plotting and discussions. Assistance in manuscript preparation from Stephanie Gallegos and enthusiastic typing support from Bonnie S. Beckner is gratefully acknowledged. Prem C. Pandey thanks the National Research Council for his associateship at Jet Propulsion Laboratory.

Dr. Pandey is on leave from the Space Applications Centre, Ahmedabad-380053, India. Mr. Kniffen is currently attending Texas A. and M. University, College Station, Texas.

REFERENCES

Bernstein, R.L., 1982: Sea surface temperature mapping with the Seasat Microwave Radiometer, J.G.R. (submitted)

Chahine, M.T., H.H. Aumann, and F.W. Taylor, 1977: Remote sounding of cloudy atmospheres. III Experimental Verifications, J. Atm. Science, 45, 758-765

Fritz, S., and J.S. Winston, 1962: Synoptic use of radiation measurements from space TIROS II. Mon. Wea. Rev., 90, 1-9

Furnival, G.M., and R.W. Wilson, Jr., 1974: Regressions by leaps and bounds, Technometrics, 16, 499-511

Gloerson, P., and F.T. Barath, 1977: A scanning multichannel microwave radiometer for Nimbus-G and Seasat-A, J. of Oceanic Eng., OE-2, 172-178

Grody, N.C., 1976: Remote sensing of atmospheric water content from satellites using microwave radiometry, IEEE Trans. Antennas Propogat., AP-24, 155-162

Green, P.E. and J.D. Carrol, 1978: Analyzing Multi-variate Data; The Dryden Press, Hinsdale, Illinois, U.S.A., pp 226-230

Hofer, R., E.G. Njoku, and J.W. Waters, 1981: Microwave radiometric mesurements of sea surface temperature from Seasat satellite: first results, Science, 212, 1385-1387

Hofer, R., and E.G. Njoku, 1981: Regression Techniques for oceanographic parameter retrieval using space-borne microwave radiometry, IEEE Geoscience and Remote Sensing, GE-19, 178-189

Lipes, R.G. Editor, 1980: JASIN Workshop Report, SMMR Panel Report, Jet Propulsion Laboratory, Pasadena, CA

Lipes, R.G., and G.H. Born, 1981: SMMR Mini Workshop IV, Jet Propulsion Laboratory, Pasadena, CA

Namias, J., 1972: Space scales of sea surface temperature anomalies and their causes, Fish. Bull., 70, 611-617

Njoku, E.G., E.J. Christensen, and R.E. Cofield, 1980a: The Seasat Scanning Multichannel Microwave Radiometer (SMMR): Antenna pattern corrections - development and implementation, IEEE J. of Oceanic Eng., OE-15, 125-137

Njoku, E.G., J.M. Stacey, and F.T. Barath, 1980b: The Seasat Scanning Multichannel Microwave Radiometer (SMMR): Instrument description and performance, IEEE J. of Oceanic Eng., OE-5, 100-115

Pandey, P.C. and R.K. Kakar, 1982a: A two step statistical technique for retrieval of geophysical parameters from microwave radiometric data. IEEE Geoscience and Remote Sensing (in press)

Pandey, P.C. and R. K. Kakar, 1982b: An empirical microwave emissivity model for a foam covered sea, IEEE J. of Oceanic Eng., OE-7, 135-140

Pandey, P.C., A.K. Sharma, and B.S. Gohlil, 1981: A simulation technique for the determination of atmospheric water content with Bhaskara Satellite Microwave Radiometer (SAMIR), Proc. Ind. Acad. of Sciences (Earth Planet Sci.), 90, 105-110

Rosenkranz, P.W., 1978: Inversion of data from diffraction - limited multiwavelength remote sensors, 1. linear case, Radio Science, 13, 1003-1010

Shukla, J., 1975: Effect of Arabian sea surface temperature anomaly on Indian summer monsoon; a numerical experiment with GFDL model, J. Atm. Science, 32, 503-511

Smith, W.L., 1978: Processing and utilization of satellite sounding data in meteorological research, Proc. Symp. use of satellite data in meteorological research, WMP, Tokyo, 108-115

Staelin, D.H., K.F. Kunzi, R.L. Pettyjohn, R.K.L. Poon, R.W. Wilcox, and J.W. Waters, 1976: Remote sensing of atmospheric water vapor and liquid water with the Nimbus-5 Microwave Spectrometer, J. Appl. Met., 15, 1204-1214

Swanson, P.N. and A.L. Riley, 1980: The Seasat Scanning Multichannel Microwave Radiometer (SMMR): Radiometric calibration algorithm development and performance, IEEE J. of Oceanic Eng., OE-5, 116-124

Waters, J.W., K.F. Kunzi, R.L. Pettyjohn, R.K.L. Poon, and D.H. Staelin, 1975: Remote sensing of atmospheric temperature profiles with Nimbus-5 microwave spectrometer, J. Atm. Sci., 32, 1953-1969

Wentz, F.J., 1982: Model function for ocean microwave brightness temperature, J. Geophys. Res. (in press)

Wilheit, T.T., and A.T.C. Chang, 1980: An algorithm for retrieval of ocean surface and atmospheric parameters from the observations of the Scanning Multichannel Microwave Radiometer, Radio Science, 15, 525-544

APPENDIX

Chester's Sea Surface Temperature Algorithm

The starting point is the linearized dependence of the T_B's for 6.6 GHz for wind speeds greater than 7 m/s supplied by Tom Wilheit:

$$T_B(6.6V) = 160 + 0.52(SST - 286K) + 0.73(W - 21\ m/s) + 0.1(V - 2.4\ g/cm^2) + 0.05(C - 20\ mg/cm^2) + 1.9(\theta - 49°)$$

$$T_B(6.6H) = 105 + 0.33(SST - 286K) + 1.52(W - 21\ m/s) + 0.1(V - 2.4\ g/cm^2) + 0.07(C - 20\ mg/cm^2) - 0.2(\theta - 49°)$$

where W = wind speed, V = column density of water vapor, C = column density of liquid water (cloud), and θ = incidence angle. Let

$$T_B'(6.6V) = T_B(6.6V) - 160 - 0.1(V - 2.4) - 0.05(C - 20) - 1.9(\theta - 49)$$

$$T_B'(6.6H) = T_B(6.6H) - 105 - 0.1(V - 2.4) - 0.07(C - 20) + 0.2(\theta - 49)$$

Then

$$T_B'(6.6V) = 0.52(SST - 286) + 0.73(W - 21)$$

$$T_B'(6.6H) = 0.33(SST - 286) + 1.52(W - 21)$$

These two equations can be inverted to yield

$$SST = 286 + 2.77\ T_B'(6.6V) - 1.33\ T_B'(6.6H)$$

$$W = 21 - 0.60\ T_B'(6.6V) + 0.95\ T_B'(6.6H)$$

Considering only SST and expanding,

$$SST = 254.62 + 2.77\ T_B(6.6V) - 1.33\ T_B(6.6H) - 5.53\theta - 0.05C - 0.14V$$

An improved estimate of SST was obtained by fitting two constants to 17 XBTs taken during Rev 1223 in the NW Pacific, giving

$$SST' = \frac{SST}{1.203} + 55.89$$

Thus, the final equation used for SST (dropping the prime) is

$$SST = 267.54 + 2.303\ T_B(6.6V) - 1.106\ T_B(6.6H) - 4.597\theta - 0.042C - 0.116V$$

The cloud and vapor formulae are given in SMMR Mini-Workshop IV report (Lipes and Born, 1981) later, although the vapor formula used in the SST algorithm does not reflect the last small change made to it. When substituted into the above,

$$SST = 257.74 + 2.303\ T_B(6.6V) - 1.106\ T_B(6.6H) - 4.461\theta$$
$$+ 1.343\ \ln(280 - T_{18V}) - 6.210\ \ln(280 - T_{18H})$$
$$- 1.392\ \ln(280 - T_{21V}) - 0.329\ \ln(280 - T_{21H})$$
$$+ 6.463\ \ln(280 - T_{37V}) + 1.522\ \ln(280 - T_{37H})\ \text{(kelvins)}$$

These formulae are valid for columns 1-3. For column 4, a bias correction of 2.6 K is added to the above formulae.

NASA—JPL—Coml., L.A., Calif.